Chapter 2

# Performance Analysis of FSO Systems over Atmospheric Turbulence Channel for Indian Weather Conditions

Prabu Krishnan

Additional information is available at the end of the chapter

http://dx.doi.org/10.5772/intechopen.80275

**Abstract**

Free-space optical (FSO) communication is a line of sight (LOS) technology and has significant advantages and attractive applications. Recently, spectrum slicing wavelength division multiplexing (SS-WDM)-based FSO systems provide improved link range, high capacity, and efficiency. In this chapter, the SS-WDM-based FSO system is proposed with four channels to increase the performance of communication under various wind speed and heights of the buildings. But, atmospheric turbulence fading, scintillation, and pointing errors (PE) are the main impairments affecting the performance of FSO communication systems. Predominantly, the turbulence variation due to wind velocity, refractive index, and height of buildings has been majorly focused and analyzed for Vellore weather conditions. A case study has been experimented on how the height of buildings and the atmosphere around VIT, Vellore campus, affect the transmission of light in free space. The bit error rate of the proposed system is analyzed with distance, received power for various wind speed and different heights of the buildings.

**Keywords:** free space optics, spectrum slicing wavelength division multiplexing (SS-WDM), bit error rate, atmospheric turbulence

## 1. Introduction

Free space optics (FSO) is an emerging and promising technology for next-generation wireless communication applications like short-range indoor wireless communication, back-haul for wireless cellular networks, last mile access, high-definition television (HDTV) transmission, and laser communications in space. In comparison with traditional radio frequency communications, the attractive features in the FSO communications include license-free operation, simple deployment, high data rate, and high transmission security [1].

However, the performance of FSO communication systems is extremely dependent of the atmospheric weather conditions. When the atmospheric channel conditions are poor, then a transmitted light signal is affected by scattering, absorption, and turbulence. The inhomogeneity in the temperature, pressure, and wind speed over the channel varies the refractive index of the atmosphere and it creates the optical signal intensity fluctuation. The negative impacts of turbulence include scintillations, phase-front distortions, beam spreading, and beam wander [2, 3]. Another significant problem with FSO links is that they are relying on the pointing performance. Errors in tracking systems, mechanical misalignment, and vibrations of the transmitter beam due to building sway phenomena lead to further performance degradation as a result of pointing errors (PE) [4].

The effects of atmospheric turbulence can be mitigated by performing aperture averaging or employing diversity at the receiver. Introducing multiple apertures at the transmitter/or the receiver provides the multiple-input multiple-output (MIMO) FSO systems potentially have to enhance performance of the system. The various forms of diversity schemes are temporal, spatial, and wavelength [5]. Relay-assisted communication is the alternate way to reduce the effects of turbulences [6]. In order to overcome this issue, certain techniques like SS-WDM were implemented. It offers high spectral efficiency and a wide coverage area which facilitates more number of users. It is a scalable network which marks its specialty in the optical networking communication area [7].

Spectrum slicing technique is used to modulate the optical signals. The desired spectrum is being sliced differently in order to modulate the optical signals accordingly and analyze the spectrum with the respective parameters [8]. Parallel transmission of slicing from a single broadband noise source has highest potential for creating a multichannel system. Spectrum slicing has a higher potential for future fiber to home access network which can further be incorporated in any optical system where low power consumption is preferred [9].

## 2. System model

The transmitter section comprises pseudo-random bit sequence (PRBS) generator, NRZ pulse generator, followed by Mach-Zehnder modulator (MZM) and a continuous wave laser, whereas the receiver consists an APD photodiode and a low-pass Bessel filter. Performance of the communication link is inspected using BER analyzer. PRBS generates information signal in the form of binary pulses, i.e., 1010101 and so on which are transformed to electrical signal thereby directing toward NRZ pulse generator. The conversion of binary pulses to electrical signals occurs (**Figure 1**). The WDM FSO link optimizing in this study was used and modified as details given in [10].

The output of NRZ pulse generator is given to MZM whose other input end receives input from a continuous wave laser. It converts the electrical signal to an optical signal. The signal is now boosted using an optical amplifier directly without converting to an electrical signal. The signal heads through the FSO channel in the form of narrow-beam electromagnetic wave which is received by a photodetector, converting optical to its corresponding electrical signal. Further,

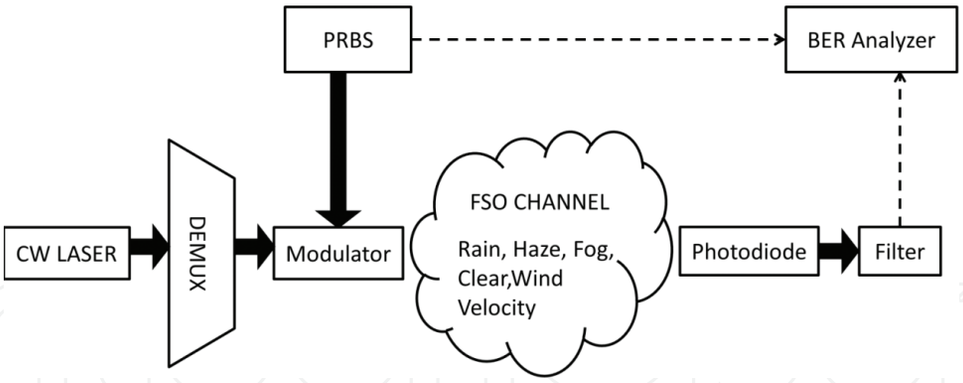


**Figure 1.** Architecture of SS-WDM-FSO communication system.

a low-pass Bessel filter suppresses the noise which is a dominant part of the signal. Desired output is achieved at the receiver which is visualized and inspected using BER analyzer [10].

## 3. Channel model

The atmospheric attenuation and turbulence are the major challenges in FSO communication system.

### 3.1. Atmospheric attenuation

The atmospheric attenuation loss modeled by Beers-Lambert law is given as [11]:

$$h_l = e^{-\sigma L} \tag{1}$$

where $\sigma$ denotes a wavelength and weather-dependent attenuation coefficient and $L$ is the propagation distance.

### 3.2. Atmospheric turbulence

The atmospheric turbulence is classified as weak, moderate, strong, and saturated regimes based on the variation of refractive index and inhomogeneity. The different mathematical models are developed to represent the turbulence regimes like log-normal, negative exponential, and gamma-gamma and M-distribution to represent weak, strong, weak-to-strong, and generalized turbulences, respectively [12–14]. The atmospheric turbulence models describe the probability density function statistics of the irradiance fluctuation.

#### *3.2.1. Lognormal*

In this model, the statistics of the irradiance fluctuations obeys the log-normal distribution. This model is characterized by a single scattering event and is best suited for weak turbulence regime. The PDF can be given as [15, 16]:

$$f(I) = \frac{1}{\sqrt{2\pi\sigma_I^2}}\frac{1}{I}\exp\left(-\frac{\left(\ln\left(\frac{I}{I_0}\right) - E[I]\right)^2}{2\sigma_I^2}\right), I \geq 0 \tag{2}$$

where $\sigma_I^2$ is the Rytov varience, I be the field irradiance in turbulent medium while the intensity in free-space (no turbulence) is represented as $I_0$, and E[I] is the mean log intensity.

*3.2.2. Negative exponential*

In this model, the number of independent scattering is very high and it can support for saturation regime. Therefore, the irradiance fluctuation follows the Rayleigh distribution entailing negative exponential statistics for the irradiance. The negative exponential PDF can be given as [15, 16]:

$$f(I) = \frac{1}{I_0}\exp\left(-\frac{I}{I_0}\right) \quad , I_0 > 0 \tag{3}$$

where $E[I] = I_0$ is the mean received irradiance.

*3.2.3. Gamma-gamma*

The atmospheric turbulence is modeled by gamma-gamma distribution with scintillation parameters $\alpha$ and $\beta$, which are indicated as functions of the Rytov variance and a geometry factor. The PDF of the gamma-gamma channel model is given by [11]:

$$f_{I_s}(I_s) = \frac{2(\alpha\beta)^{(\alpha+\beta)/2}}{\Gamma(\alpha)\Gamma(\beta)} I_s^{(\alpha+\beta)/2-1} K_{(\alpha-\beta)}\left(2\sqrt{\alpha\beta I_s}\right) \tag{4}$$

where $\alpha$ and $\beta$ are the effective number of large- and small-scale turbulent eddies, $\Gamma(\cdot)$ is the gamma function, and $K_{(\alpha-\beta)}$ is the modified Bessel function of the second kind of order $(\alpha - \beta)$. The effective number of large- and small-scale turbulent eddies $\alpha$ and $\beta$ for a spherical wave is given by [11]:

$$\alpha = \left[\exp\left(\frac{0.49\delta_n^2}{\left(1 + 0.18d^2 + 0.56\delta_n^{12/15}\right)^{7/6}}\right) - 1\right]^{-1} \tag{5}$$

$$\beta = \left[\exp\left(\frac{0.51\delta_n^2\left(1 + 0.69\delta_n^{12/15}\right)^{-5/6}}{\left(1 + 0.9d^2 + 0.62d^2\delta_n^{12/15}\right)^{5/6}}\right) - 1\right]^{-1} \tag{6}$$

where $d = \sqrt{kD^2/4L}$, $k = 2\pi/\lambda$, is the optical wave number with $\lambda$ being the operational wavelength, L is the length of the optical link, and D is the receiver's aperture diameter. The parameter

$\delta_n^2$ is the Rytov variance and is given as: $\delta_n^2 = 0.5C_n^2k^{7/6}L^{11/6}$ and the $C_n^2$ represents the refractive index structure parameter. This model is valid for all turbulence regimes from weak to strong and the gamma-gamma distribution approaches negative exponential distribution when it approaches saturation regime [17, 18].

*3.2.4. M-distribution*

The transmitted signal is scattered due to natural turbulences such as rain, fog, smoke, smog, and heavy dust particles in the atmospheric channel (AC). The combined effects of fading due to atmospheric turbulence and misalignment are considered and the combined unconditional probability density function (PDF) for M-distribution has been derived in [19]. As derived in [19], the PDF of the irradiance $h$ is given by:

$$f_I(I) = \frac{g^2 A}{2I}\sum_{k=1}^{\beta} a_k \left(\frac{\alpha\beta}{\mu\beta+\Omega'}\right)^{-\frac{\alpha+k}{2}} G_{1,3}^{3,0}\left[\frac{\alpha\beta}{\mu\beta+\Omega'}\frac{I}{A_0}\middle|_{g^2,\alpha,k}^{g^2+1}\right] \tag{7}$$

where $\mu = 2b_0(1-\rho)$ is a large-scale scattering parameter, $\beta$ is the quantity of fading parameter, $A_0$ is the fraction of the collected power at r = 0 (radial distance), $\Omega' = \Omega + 2\rho b_0 + 2\sqrt{2\rho b_0\Omega}\,cos\left(\phi_A - \phi_B\right)$ be the average power. The amount of scattering power coupled to the LOS component is denoted by the parameter $\rho$ and its range from 0 to 1. The parameters $\phi_A$and$\phi_B$ are the deterministic phases of the LOS and the coupled-to-LOS component. The parameters $g$, $A$ and $a_k$ are defined as [19]

$$g = \frac{w_{zeq}}{2\sigma_s} \tag{8}$$

$$A = \frac{2\alpha^{\alpha/2}}{\mu^{1+\alpha/2}\Gamma(\alpha)}\left(\frac{\mu\beta}{\mu\beta+\Omega'}\right)^{\beta+\alpha/2} \tag{9}$$

$$a_k = \binom{\beta-1}{k-1}\frac{\left(\mu\beta+\Omega'\right)^{1-0.5k}}{(k-1)!}\left(\frac{\Omega'}{\mu}\right)^{k-1}\left(\frac{\alpha}{\beta}\right)^{0.5k} \tag{10}$$

where $\sigma_s$ is the pointing error displacement standard deviation at the receiver, $w_{zeq}$ be the equivalent beam radius and can be calculated by using the relations $v = \sqrt{\pi}a/\sqrt{2}w_z$, $w_{zeq} = w_z^2\sqrt{\pi}\mathrm{erf}(v)/2ve^{-v^2}$, where $w_z$ is the beam waist at distance $z$, $a$ is the radius of a circular detection aperturture. The gamma-gamma, K-distribution, and negative exponential model are obtained by the values of the parameter$(\rho = 1, \Omega' = 1)$, $\left(\rho = 0, \Omega = 0\ or\ \beta = 1\right)$, *and* $(\rho = 0, \Omega = 0\ or\ \alpha \to \infty)$, respectively.

### 3.3. Wind speed-induced turbulence

Wind control is a standout among the most essential wellsprings of feasible vitality which is sustained on a little and additionally extensive scale. It is the most noticeable factor which weakens the optical signal which propagates over free space [20]. The optical signal blurs as

the climatic visibility diminishes because of the turbulence which relates the refractive record nonhomogeneity parameter of the particles introduced in the air. In Ref. [21], the authors experimented the FSO link which is located at Milesovka hill situated 70 km north to Prague. It is been seen that flag lessening is conversely relative to meteorological visibility. The visibility at the transmitter and receiver sites is interfered by the wind speed which can be mathematically modeled using 3D vector where refractive index and rain rate are continuously recorded which estimate quantitative impact on attenuation.

Atmospheric turbulence brings about irregular change of the refractive index of the light propagation path. This refractive index change is the immediate final result of arbitrary discrepancies in atmospheric temperature from point to point [22]. These random temperature fluctuations are a function of the atmospheric pressure, altitude, and wind speed.

Wind is also persuading the received power of the FSO link signal. Wind, especially wind turbulences, causes hurdle changes of the atmosphere refractive index which is redistributing the optical beam of the FSO link. In order to investigate the wind influence on the FSO link attenuation, we selected important wind parameters influencing the FSO link attenuation due to this optical energy redistribution.

Therefore, the temperature and wind speeds are measured and the attenuation due to wind turbulence is calculated. Based on the calculated attenuation, the BER versus received power and distance is analyzed for various heights of buildings and minimum, maximum wind speeds.

The relative humidity, minimum, and maximum temperature variation during April 2017 at Vellore 12.92°N/79.13°E, 267 m is shown in **Figure 2**. The minimum and maximum temperature obtained in the month of April 2017 is 21 and 43°C. **Figure 3** illustrates the speed and direction of wind during April 2017 at Vellore, India. The direction of wind is represented using angles 0, 90, 270, and 360° for South, West, North, and East, respectively. The minimum and maximum speed of wind recorded in the month of April 2017 is 2.5 and 26 km/h.

The atmospheric turbulence because of wind speed introduces radical fluctuations in refractive index that affects the propagation FSO signal [23]. In order to analyze the influence of wind on

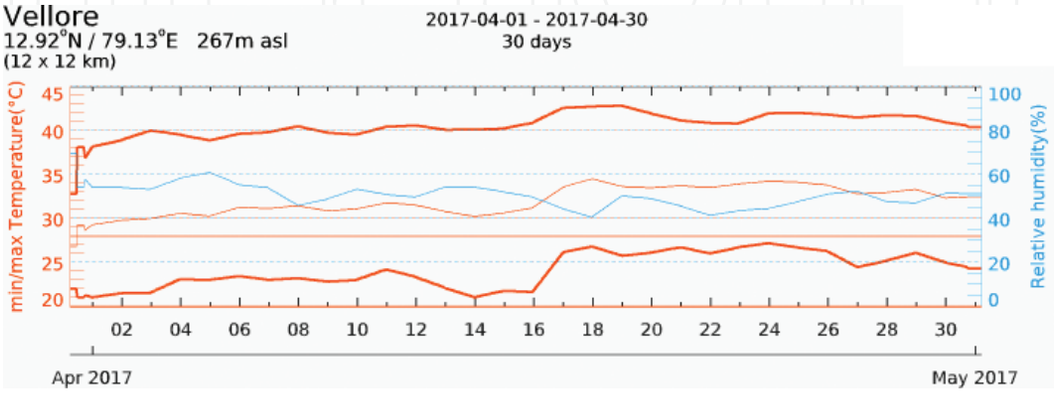


**Figure 2.** Temperature and relative humidity during April 2017 at Vellore, India [23].

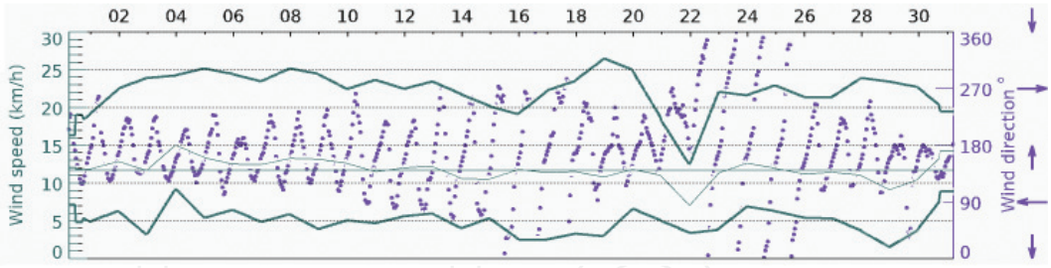


**Figure 3.** Wind speed and direction during April 2017 at Vellore, India [23].

FSO system, the turbulent energy, direction, and velocity of the wind have to be considered. The turbulent energy of the wind at every direction can be calculated as:

$$E_t = \frac{1}{2N}\sum\left[(x-\overline{x})^2 + (y-\overline{y})^2 + (z-\overline{z})^2\right] \tag{11}$$

where $\overline{x}$, $\overline{y}$, $\overline{z}$ are the given wind speeds in a particular direction, x, y, z are the cumulative wind speed in any one direction, N be the number of samples, and $E_t$ is the turbulent energy. The turbulent energy represents wind velocity standard deviation. The attenuation caused by the turbulence can be calculated by a regressive formula which is as follows:

$$\mathrm{A} = 70 - 73e^{-0.2867\mathrm{Et}} \tag{12}$$

## 4. Results and discussion

The BER of the proposed system is analyzed with respect to transmission distance and received power over various wind speeds and different heights of buildings. The results are compared with and without spectrum slicing-based WDM FSO system. It shows the importance of spectrum slicing in WDM-based FSO systems.

This imparts that wind speed in any direction can be correlated to FSO link attenuation. Since the wind speed affects the propagation of the signal, the height of the buildings also obstructs the signal transmission. The analysis on how the heights of buildings play a significant role is deeply inspected in VIT University, Vellore, Tamil Nadu, India. The wind speed velocities have been captured during the month of April 2017. The current status of the wind has viewed from meteorological media which gives the flow of wind in every direction. This assists in calculating the exact direction of wind and has been analyzed using Eqs. (11) and (12) respectively. The attenuation values have been calculated for maximum and minimum values of the wind speed. The buildings in VIT for which it has been experimented are Technology Tower (TT), Silver Jubilee Tower (SJT), GDN, and Rajeswari Tower, which have the range of heights from 10 to 50 m. The graphs have been plotted in order to analyze the effect of turbulence on the FSO link with building heights of 10 and 80 m. In Vellore region, July to September is the monsoon season. So, we have considered the rain data from July to September.

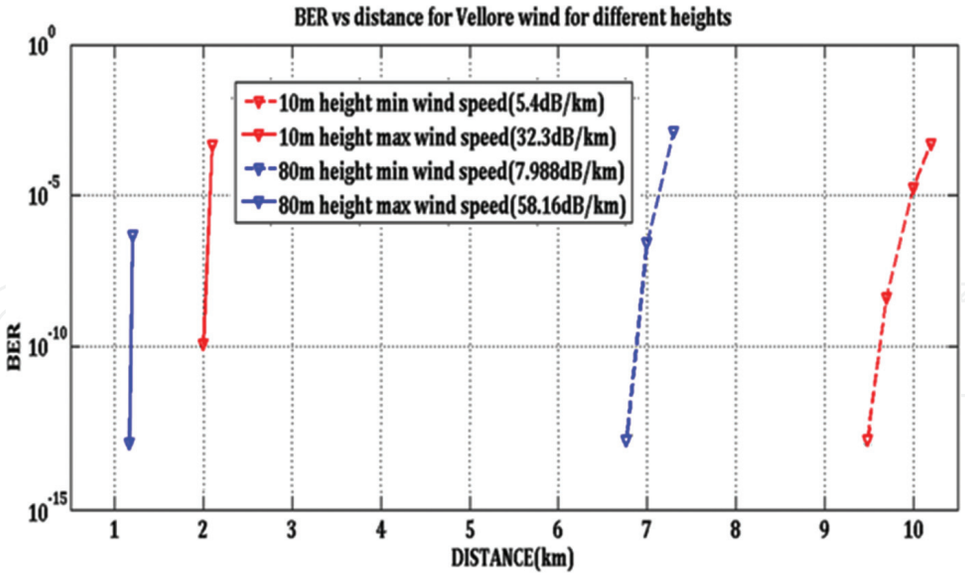


**Figure 4.** BER in terms of distance for Vellore weather conditions affected by wind velocity and building heights.

The BER in terms of transmission distance for four-channel SS-WDM FSO system is illustrated in **Figure 4**. The error rate performance is analyzed with respect to various building heights, minimum and maximum wind speed. From the figure, it is observed that at a height of 10 m, the BER of $10^{-10}$ is achieved at 9 km distance under minimum wind speed. But, for the same height the same BER can be achieved only at the link range of 2 km under maximum wind speed. That is, the wind speed decreases the link range about 7 km from the analysis. At 80 m height, the minimum BER of $10^{-13}$ is achieved at 7 and 1 km over minimum and maximum wind speed, respectively. It is inferred that at both heights, the speed of wind decreases the link range of an FSO system.

The BER versus received power shown in **Figure 5** is the received power analysis done in Vellore, Tamil Nadu, India. It shows how the received power of an FSO link is affected by building heights at various wind velocities. As we expected that the received power increases, the BER decreases. From the figure, it is observed that at a height of 10 m, near the received power of −70 dBm under influence of minimum wind speed, the BER recorded is $10^{-9}$. Near the received power of −72 dBm, spectrum slicing gives a qualitatively better BER value of $10^{-6}$ when the building height is 80 m for maximum wind speed.

In forest area due to high evapotranspiration, that is, the water from the plants, trees, and land surface are transferred to the atmosphere in the form of gas, optical signal fading will be high. Because, the phase changed water contents (gas) use to absorb the energy and cool the land surface and the end result is a high level of turbulence compared with urban areas. Wind direction can be imagined as a horizontal flow of numerous rotating eddies, that is, turbulent vortices of various sizes, with each eddy having horizontal and vertical components [24] is shown in **Figure 6**. Since the turbulence level is high, the transmitted optical signal scintillation will be more with the effects of high BER.

http://dx.doi.org/10.5772/intechopen.80275

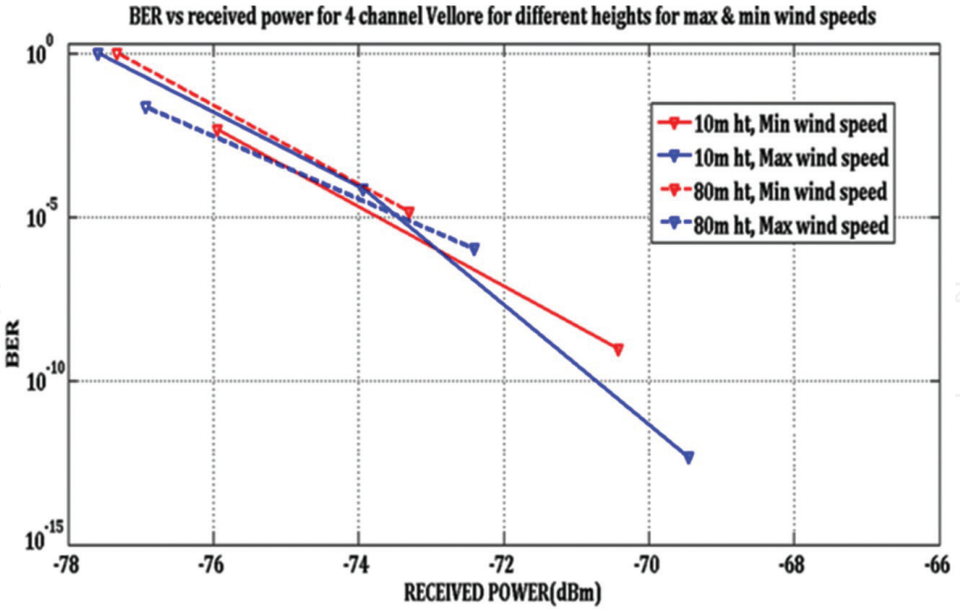


**Figure 5.** BER versus received power for Vellore weather conditions affected by wind velocity and building heights.

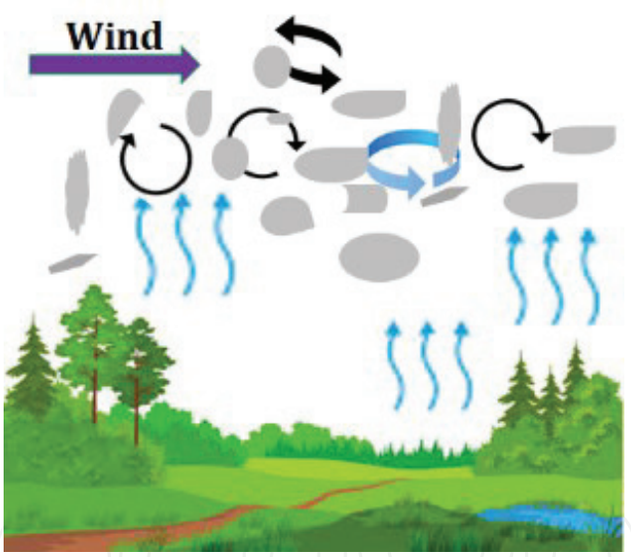


**Figure 6.** Rotation of turbulent eddies with respect to horizontal wind flow.

**Figure 7** demonstrates the BER versus distance plot for forests under the effect of wind speed at various heights of 15, 33, and 97 m for four-channel system model. At 15 m height, it is noticed that in case of SS-WDM-FSO, BER value is $10^{-10}$ at a distance of 210 km. In case of WDM-FSO, the BER is $10^{-8}$ at the same distance. For a forest height of 33 m, it is seen that a BER value of $10^{-6}$ is achieved at a distance of 10 km, when no spectrum slicing is done on the system, whereas for the same distance, BER value of nearly $10^{-7}$ is obtained when the FSO channel is subjected to slicing. So, it can be said that slicing the channel does give a considerable amount of change in BER values. For forest with tree heights around 97 m under influence

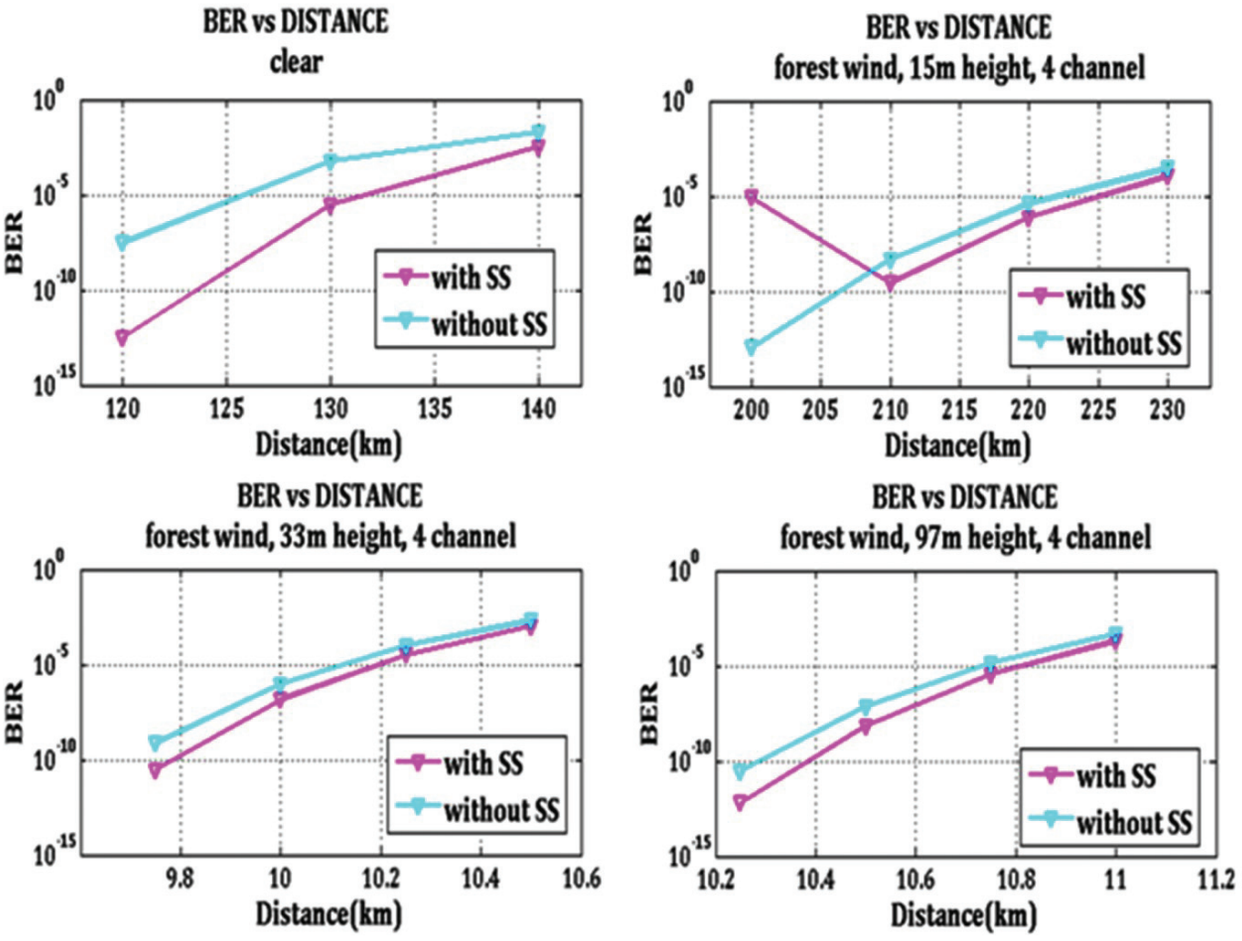


**Figure 7.** BER in terms of distance for forests under influence of wind speeds at various heights of 15, 33, and 97 m for four-channel model.

of wind, it is observed that the BER value of $10^{-10}$ is obtained at an FSO link length of 10.4 km and $10^{-8}$ at the same distance with and without slicing, respectively. This shows that a low BER value is obtained in case of spectrum slicing.

## 5. Conclusion

In this chapter, the SS-WDM FSO system is proposed and the importance of spectrum slicing on WDM FSO systems is analyzed in terms of average BER. Effect of wind velocity as well as turbulent energy on various building in VIT University has been deeply studied and results have been plotted. The performance of the SS-WDM-FSO system is analyzed for various building heights, wind speeds in terms of distance and received power. It has been observed that the wind speed and height of buildings decreases the link range of FSO system. It also affects the BER performance of the system. Also observed is that the spectrum slicing reduced the number of components and losses. It improves the spectrum efficiency of the system, and it is compact and cost effective.

## Author details

Prabu Krishnan

Address all correspondence to: nitprabu@gmail.com

Department of Electronics and Communication Engineering, National Institute of Technology Karnataka, Surathkal, India

## References

[1] Peppas KP, Stassinakis AN, Topalis GK, Nistazakis HE, Tombras GS. Average capacity of optical wireless communication systems over IK atmospheric turbulence channels. 2012; **4**(12):1026-1032

[2] Krishnan P, Kumar DS. Performance analysis of free-space optical systems employing binary polarization shift keying signaling over gamma-gamma channel with pointing errors. Optical Engineering. 2014;**53**(7):076105-076105

[3] Prabu K, Sriram Kumar D. MIMO free-space optical communication employing coherent BPOLSK modulation in atmospheric optical turbulence channel with pointing errors. 2015;**343**:188

[4] Sandalidis HG. Coded free-space optical links over strong turbulence and misalignment fading channels. IEEE Transactions on Communications. 2011;**59**(3):669-674

[5] Bayaki E, Schober R, Mallik R. Performance analysis of MIMO free-space optical systems in gamma–gamma fading. IEEE Transactions on Communications. 2009;**57**(11):3415-3424

[6] Laneman JN, Tse DNC, Wornell GW. Cooperative diversity in wireless networks: Efficient protocols and outage behavior. 2004;**50**(12):3062-3080

[7] Prabu K, Sriram Kumar D. BER analysis of DPSK–SIM over MIMO free space optical links with misalignment. Optik. 2014;**125**(18):5176-5180

[8] Aladeloba AO, Woolfson MS, Phillips AJ. WDM FSO network with turbulence-accentuated interchannel crosstalk. 2013;**5**(6):641-651

[9] Ciaramella E, Arimoto Y, Contestabile G, Presi M, D'Errico A, Guarino V, Matsumoto M. 1.28 Terabit/s (32 × 40 Gbit/s) WDM transmission system for free space optical communications. IEEE Journal on Selected Areas in Communications. 2009;**27**(9):1639-1645

[10] Prabu K, Charanya S, Jain M, Guha D. BER analysis of SS-WDM based FSO system for Vellore weather conditions. Optics Communications. 2017;**403**:73-80

[11] Andrews LC, Phillips RL. Laser Beam Propagation through Random Media. Bellingham: SPIE Press; 2005

[12] Killinger D. Free space optics for laser communication through the air. 2002;**13**:36-42

[13] Nistazakis HE, Karagianni EA, Tsigopoulos AD, Fafalios ME, Tombras GS. Average capacity of optical wireless communication systems over atmospheric turbulence channels. 2009; **27**:974-979

[14] Nistazakis HE, Tsiftsis TA, Tombras GS. Performance analysis of free-space optical communication systems over atmospheric turbulence channels. IET Communications. 2009;**3**: 1402-1409

[15] Ghassemlooy Z, Popoola W, Rajbhandari S. Optical Wireless Communications System and Channel Modelling with MATLAB. Boca Raton, Florida's: CRC Press; 2012

[16] Ghassemlooy Z, Tang X, Rajbhandari S. Experimental investigation of polarisation modulated free space optical communication with direct detection in a turbulence channel. IET Communications. 2012;**6**:1489-1494

[17] Garrido-Balsells JM, Jurado-Navas A, Paris JF, Castillo-Vázquez M, Puerta-Notario A. On the capacity of $\mathcal{M}$-distributed atmospheric optical channels. Optics Letters. 2013;**38**(20): 3984-3987

[18] Tang X, Xu Z, Ghassemlooy Z. Coherent polarization modulated transmission through MIMO atmospheric optical turbulence channel. 2013;**31**(20):3221-3228

[19] Yang L, Hasna MO, Gao X. Asymptotic BER analysis of FSO with multiple receive apertures over $\mathcal{M}$-distributed turbulence channels with pointing errors. Optics Express. 2014;**22**(15):18238-18245

[20] Turbulence Intensity in Complex Environments and its Influence on Small Wind Turbines. Uppsala, Sweden: Nicole Carpman; 2011

[21] Fiser O et al. FSO link attenuation measurement and modelling on Milesovka hill. In: Proceedings of the 5th European Conference on Antennas and Propagation (EUCAP). Rome, Italy: IEEE; 2011

[22] Pratt WK. Laser Communication Systems. 1st ed. New York: John Wiley & Sons, Inc.; 1969

[23] https://www.meteoblue.com/en/weather/forecast/week/vellore_india_1253286 (Data for wind speed)

[24] Wang K, Dickinson RE. A review of global terrestrial evapotranspiration: Observation, modeling, climatology, and climatic variability. Reviews of Geophysics. 2012;**50**(2):1-54